**EUROPEAN LABORATORY FOR PARTICLE PHYSICS**

**CERN - SL Division**

SL-RFS Note 91-14
LHC Note 175

# THE TRANSVERSE DAMPER SYSTEM FOR LHC

V.M. Zhabitsky [1)]

## Abstract

A transverse damper system with an IIR-filter (infinite impulse response filter) in the feedback circuit is proposed for the LHC. It consists of one pick-up and one damper kicker in each plane of beam transverse oscillations. The pick-up and the kicker are connected by a feedback circuit including a delay and a digital IIR-filter which removes the revolution frequency harmonics from the pick-up signal. The Fourier transform is used to study the coasting beam dynamics with resistive wall instability. The analytical solutions for the damping time and for the eigen frequencies have been obtained and the system stability analyzed.

---

1) Joint Institute for Nuclear Research, Dubna, USSR

13 December 1991

## 1 INTRODUCTION

In this article the transverse damper system for LHC [1] will be discussed. For a large part this proposal is based on the theoretical studies of the transverse damper system for the First Stage of UNK [2-7]. The UNK damper system will be used to suppress a very strong resistive wall instability. This fast instability is caused by the large real part of the transverse coupling impedance of the conventional (non superconducting) ring for the First Stage of UNK [2]. In order to suppress this fast resistive wall instability a more effective system has been designed and developed [4-7]. It consists of two pick-ups and two kickers in each plane of beam transverse oscillations.

In the LHC case, where most of the ring is superconducting, the real part of the transverse coupling impedance is not as large as for the UNK conventional ring. For this reason a classical transverse damper system is proposed for LHC. This system consists of one pick-up and one damper kicker per plane connected by a feedback circuit including a digital filter and delay. Similar systems have been used in many accelerators (see, for example, [8,9]). To remove the revolution frequency harmonics notch filters have been included in the feedback circuits of the damper systems. They could be built with the FIR-filter (finite duration impulse response filter) technology [8,9]. But IIR-filters (infinite duration impulse response filter) give better results for a damper system [7,10] and for this reason an IIR-filter is proposed for the LHC. In this article the system stability with a digital IIR-filter will be analyzed.

## 2 THE RESISTIVE WALL INSTABILITY PARAMETERS IN LHC

The resistive wall instability in large proton accelerators and colliders is particularly important because of the low particle revolution frequency. The real part of the transverse coupling impedance $ReZ_T(\omega)$ increases at low frequency and so does the growth rate (or increment) of the instability. It is known [2,11] that the resistive instability rise time is given by:

$$\tau_r = \frac{2C_0 mc\gamma}{eI} \frac{1}{\beta_{av} ReZ_T(\omega)} , \qquad (1)$$

where $C_0$= 26658.87 m, circumference of the closed orbit;

$mc^2\gamma$ - proton total energy; $\beta_{av}$= 82.5 m - average $\beta$-function [1]. The total beam current I is

$$I = eK_bN_b/T_0, \qquad (2)$$

where $K_b$= 4725, number of bunches; $N_b$= $10^{11}$- number of particles per bunch; $T_0$= 88.92 $\mu$s, revolution period. Thus, I = 850 mA in the LHC.

The real part of the transverse coupling impedance is [2,11]:

$$ReZ_T(\omega) = \frac{C_0Z_0}{2\pi b^2}\cdot\begin{cases} \delta/b & \text{for } \delta \ll \Delta, \\ \delta^2/b\Delta & \text{for } \delta \gg \Delta. \end{cases} \qquad (3)$$

Here $Z_0$= $\mu_0 c \simeq 377\ \Omega$, impedance of free space; b - beam pipe radius (we assume b = 1.3 cm, i.e. half of the full height of the elliptic vacuum chamber); $\Delta$ = 2 mm, beam tube thickness. The skin depth $\delta$ for a tube with resistivity $\rho$ is given by:

$$\delta(\omega) = \sqrt{\frac{2\rho}{\mu_0\omega}}\ . \qquad (4)$$

It is easy to see that for high frequencies, when $\delta \ll \Delta$, the real part of the transverse coupling impedance is proportional to $1/\sqrt{\omega}$, but for low frequencies, when $\delta \gg \Delta$, we have $ReZ_T \approx 1/\omega$. Hence, the resistive instability is a very dangerous effect at low frequencies when the electromagnetic field penetrates through the wall of the beam tube [2].

The lowest frequency for the resistive wall instability is

$$\omega_{min} = \min|k \pm ReQ|, \qquad (5)$$

where k is an integer (positive or negative); Q is a complex quantity, depending on $\omega$, the real part of which is equal the machine tune. For LHC we have

$$(\omega_{min}/2\pi) \simeq 0.3f_0 \simeq 3.37\ kHz.$$

It is assumed that about 90% of the machine circumference will be at liquid-helium temperature [1]. The resistivity $\rho_c$ of copper at this temperature is lower than at room temperature and, in the presence of the injection magnetic field, the effective resistivity determined by the magnetoresistance effect is $\rho_c$= $0.8\cdot 10^{-10}\Omega\cdot m$. For this $\rho_c$ the skin depth $\delta_c(\omega_{min})$ is 0.08 mm.

About 10% of the beam tube will be at room temperature where the resistivity is larger. At low frequency the skin depth of copper is 1.1 mm ($\rho$ = $1.72\cdot 10^{-8}\Omega\cdot m$) whereas the skin depth of stainless steel with resistivity $\rho_r$= $9.1\cdot 10^{-7}\Omega\cdot m$ is $\delta_r(\omega_{min})$= 8.3 mm. It has been proposed to use a stainless steel beam tube with a thickness $\Delta = 2$ mm [1]. This means that $\delta_r(\omega_{min})$ will be greater than the beam tube thickness.

Hence, for the LHC parameters we get from (3):

$$ReZ_T(\omega_{min}) = 9.46 \cdot 10^9 (0.9\delta_c/b + 0.1\delta_r^2/b\Delta) =$$
$$= 9.46 \cdot 10^9 (5.4 \cdot 10^{-3} + 0.263) = 2.5 \cdot 10^9 \Omega/m. \qquad (6)$$

It easy to see that the main part of the LHC transverse impedance is determined by the beam tube at room temperature.

For the resistive instability rise time we have from (1):

$$\tau_r = 0.45 \text{ ms}.$$

Hence, the imaginary part of Q equals

$$|ImQ| = T_0/2\pi\tau \cong 0.03. \qquad (7)$$

If we use a beam tube made of thick copper, the electromagnetic field will not penetrate through the wall. In this case we have for $\delta_r = 1.1$ mm:

$$ReZ_T(\omega_{min}) = 9.46 \cdot 10^9 (0.9\delta_c/b + 0.1\delta_r/b) = 1.3 \cdot 10^8 \Omega/m.$$

In the case of a stainless steel beam tube with a thickness $\Delta > \delta_r = 8.3$ mm, we obtain:

$$ReZ_T(\omega_{min}) = 9.46 \cdot 10^9 (0.9\delta_c/b + 0.1\delta_r/b) = 6.6 \cdot 10^8 \Omega/m.$$

To cover these cases where $ReZ_T$ is approximately 20 or 4 times smaller than in (6) we propose another estimate for the imaginary part of Q:

$$|ImQ| \cong 0.01. \qquad (8)$$

These two values for ImQ ($|ImQ| = 0.03$ and $|ImQ| = 0.01$) will be used for the simulation of the transverse damper system for LHC.

## 2 THE STRUCTURE OF THE DAMPER SYSTEM

The transverse damper system will be used:

- for damping the injection oscillations of bunches immediately after injection from the SPS,
- for suppression of the transverse resistive wall instability of the intense beams in LHC,
- for damping of other coupled bunch transverse instabilities which might be induced by narrow band impedances.

A schematic diagram of the damper system for one beam is shown in Figure 1. The damper includes one pick-up (PU) and one damper kicker (DK) connected by negative feedback circuit with delay. The signal $V_{in}$ from the PU is proportional to the beam displacement $x_p$ at the PU location. The PU sensitivity is $S_p = V_{in}/x_p$. The signal from the PU is transmitted to the preamplifier with gain $K_{in}$ and to the filter with gain $K_f$. The filter is used to suppress the revolution frequency harmonics. The signal from the filter is amplified through the power amplifier with gain $K_{out}$ and sent to the kicker DK with a transfer characteristic $S_K$. After the kicker the angle of the beam is changed by $\Delta x'_K = S_K V_{out}$ but the beam deviation will be the same (it is true for a short damper kicker). The kicker should change the angle of the same fraction of the beam that was measured by the PU. The delay $\tau$ is adjusted to provide such a synchronization. Thus, the damper kicker corrects the beam angular error according to the beam deviation from the PU electrical center at the pick-up location every turn.

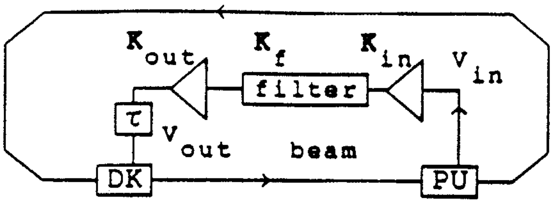

Fig.1

The Fourier components of the signals can be written:

$$\tilde{V}_{out}(\omega) = K_V(\omega)\exp(-j\omega\tau)\tilde{V}_{in}(\omega),$$

where $K_V(\omega) = K_{in}K_f K_{out}$ and $\tau$ is the delay in the feedback circuit. For the $\Delta x'_K$ and $x_p$ Fourier components we have:

$$\Delta\tilde{x}'_K = \frac{1}{\sqrt{\beta_p\beta_K}} K_T(\omega)\exp(-j\omega\tau)\tilde{x}_p; \qquad K_T(\omega) = \sqrt{\beta_p\beta_K}\, S_K S_p K_V(\omega), \qquad (9)$$

where $\beta_p$ and $\beta_K$ are the $\beta$-functions at the PU and DK locations. The gain factor $K_T(\omega)$ will be used further in all formulas.

The problem is now to define the region of $K_T(\omega)$ in the complex plane where the particle motion is stable.

## 3 THEORY OF A CLASSICAL TRANSVERSE DAMPER SYSTEM WITH A FILTER IN THE FEEDBACK PATH

In this part of the article we shall use the theory of a transverse damper system with a filter in the feedback path developed in [7]. There the Fourier transform approach is used to study the damper system for a coasting beam. After complete injection from SPS to LHC the beam almost fully occupies the machine circumference, and therefore the model of a coasting beam will also be used in LHC.

For the beam dynamic equation of the transverse coherent motion we shall use the equation from [3,7]. Let $x_c(t,s)$ be the coasting beam deviation from the closed orbit at the time $t$ and at the point $s$ of circumference. The deviation $x_c(t,s)$ is understood in the hydrodynamics sense. This means that at a certain time $t$ the different values of $s$ correspond to different particles for this particular $t$ and the function $x_c(t=\text{const},s)$ describes the particle distribution at the moment $t$. If $s = \text{const}$ then at this position we shall see the deviation of different particles as time proceeds. Due to the periodicity of $s$ in the circular accelerator we can write

$$x_c(t,s+C_0) = x_c(t,s); \qquad x'_c(t,s+C_0) = x'_c(t,s). \tag{10}$$

In accordance with [3,7] we can write for $x_c(t,s)$

$$\left[\left(\frac{1}{v_0}\frac{\partial}{\partial t} + \frac{\partial}{\partial s}\right)^2 + K(s)\right]x_c(t,s) =$$
$$= \int_0^t \Delta K_B(t-t')x_c(t',s)dt' + F(s) + F_K(t)\delta(s-s_K), \tag{11}$$

where $K(s)=K(s+C_0)$ is the focusing strength; $v_0$- the particle longitudinal velocity on the closed orbit. The space charge forces and the effects of the walls on the coherent beam motion are described by an integer operator with kernel $\Delta K_B(t-t')$. Such a description of the Lorentz force corresponds to the quasi static approximation for the electromagnetic field. This model is usually applied for the description of the resistive wall instability of a coasting beam.

The perturbation function $F(s)$ describes the influence of the errors in the magnetic guide field on the closed orbit. The function $F_K(t)$ characterizes the feedback effect on the particle motion at the DK location $s_K$ and at the time t. For the feedback in Fig.1 we can write

$$F_K(t) = \int_0^t K_{KP}(t-t')x_c(t',s_P)dt', \tag{12}$$

where $s_P$- the PU location on the closed orbit.

For time dependent functions in Eq.(11) we can calculate the one-side Fourier (Laplace) transform. Using (12) and (9), after simple transformations we get

$$\left[\frac{d^2}{ds^2} + \tilde{K}_B(s,\omega)\right]\tilde{y}(\omega,s) = \left[v_0^{-2}\left(j\omega x_c(0,s) + \dot{x}_c(0,s)\right) + \frac{F(s)}{j\omega}\right]\exp\left(\frac{j\omega s}{v_0}\right) +$$

$$+ \frac{1}{\sqrt{\beta_P\beta_K}} K_T(\omega)\exp\left(j\omega(\tau_{PK}-\tau)\right)\ \tilde{y}(\omega,s_P)\delta(s-s_K), \tag{13}$$

where $\tilde{K}_B(s,\omega) = K(s)-\Delta\tilde{K}_B(\omega)$. During the transformation we introduced a new function $\tilde{y}(\omega,s)$ instead of the Fourier component of $x_c(t,s)$:

$$\tilde{x}_c(\omega,s) = \int_0^\infty x_c(t,s)\exp(-j\omega t)dt = \tilde{y}(\omega,s)\exp(-j\omega s/v_0). \tag{14}$$

The functions $x_c(0,s)$ and $\dot{x}_c(0,s) = \partial x_c(0,s)/\partial t$ in Eq.(13) describe the particle distribution at the initial moment t=0. The particle time of flight between PU and DK is

$$\tau_{PK} = (s_K-s_P)/v_0. \tag{15}$$

Due to the periodicity on $s$ (10) we have for $\tilde{y}(\omega,s)$:

$$\tilde{y}(\omega,s+C_0) = \tilde{y}(\omega,s)\exp(j\omega T_0). \tag{16}$$

We recognize in the left hand side of Eq.(13) the same form as an usual betatron equation for a single particle. But we must emphasize that $\tilde{K}_B(s,\omega)$ is here a complex value and differs from K(s) by $\Delta\tilde{K}_B(\omega)$ due to space charge effects.

The particular solution for Eq.(13) consists of two parts. The first one is $\tilde{y}_{f0}(\omega,s)$ and takes into account the initial particle distribution at t=0 and the perturbation force F(s). The second one is $\tilde{y}_K(\omega,s)$ and depends on the kicker effect of the feedback. The first solution is

$$\tilde{y}_{f0}(\omega,s) = \int_{s_0}^{s}\left[v_0^{-2}\left(j\omega x_c(0,s') + \dot{x}_c(0,s')\right) + \frac{F(s')}{j\omega}\right]\exp\left(\frac{j\omega s'}{v_0}\right)\cdot$$

$$\cdot\sqrt{\beta(s)\beta(s')}\ \sin\left(\psi(s)-\psi(s')\right)ds',$$

where $\psi(s)-\psi(s')$ is the phase advance between points $s$ and $s'$ with $\beta$-function values $\beta(s)$ and $\beta(s')$. This phase advance is

$$\psi(s)-\psi(s') = \int_{s'}^{s}\frac{ds}{\beta(s)}. \tag{17}$$

It is necessary to emphasize that $\tilde{y}_{f0}(\omega,s_0)=\tilde{y}'_{f0}(\omega,s_0)=0$, where $s_0$ is an arbitrary point. For $\tilde{y}_K(\omega,s)$ we get at $s>s_K$

$$\tilde{y}_K(\omega,s) = \frac{1}{\sqrt{\beta_P\beta_K}} K_T(\omega)\exp\left(j\omega(\tau_{PK}-\tau)\right)\ \tilde{y}(\omega,s_P)\sqrt{\beta(s)\beta_K}\ \sin\left(\psi(s)-\psi(s_K)\right).$$

The general solution of Eq.(13) can be written in matrix form as the solution of the homogeneous equation with the initial state $\hat{y}_0(\omega,s_0)$ plus the particular solutions $\hat{y}_{f0}(\omega,s)$ and $\hat{y}_K(\omega,s)$ for the inhomogeneous equation:

$$\hat{y}(\omega,s)=\hat{M}(\omega;s,s_0)\hat{y}_0(\omega,s_0)+\hat{y}_{f0}(\omega,s)+\hat{y}_K(\omega,s),$$

where

$$\hat{y}_0(\omega,s_0)=\begin{pmatrix}y_0(\omega,s_0)\\ y_0'(\omega,s_0)\end{pmatrix};\qquad \hat{y}_{f0}(\omega,s)=\begin{pmatrix}\tilde{y}_{f0}(\omega,s)\\ \tilde{y}_{f0}'(\omega,s)\end{pmatrix};\qquad \hat{y}_K(\omega,s)=\begin{pmatrix}\tilde{y}_K(\omega,s)\\ \tilde{y}_K'(\omega,s)\end{pmatrix}.$$

The matrix $\hat{M}(\omega;s,s_0)$ is an ordinary transfer matrix from point $s_0$ on the closed orbit to point s. It is not difficult to see that

$$\hat{y}_K(\omega,s_0+C_0)=\frac{1}{\sqrt{\beta_P\beta_K}}K_T(\omega)\exp\left(j\omega(\tau_{PK}-\tau)\right)\hat{D}^{-1}\hat{A}_0\hat{T}\hat{D}y_0(\omega,s_0),$$

where $\hat{A}_0$ is the transfer matrix from $s_K$ to $s_P$ (from DK to PU); $\hat{D}$ is the transfer matrix from $s_0$ to $s_P$. $\hat{T}$ is the 2x2 matrix in which $T_{21}=1$ and the other elements are zero.

Following Eq.(16) we have

$$\hat{y}(\omega,s_0+C_0)=\exp(j\omega T_0)\hat{y}(\omega,s_0)=\exp(j\omega T_0)\hat{y}_0(\omega,s_0)=$$
$$=\hat{M}_s(\omega)\hat{y}_0(\omega,s_0)+\hat{y}_{f0}(\omega,s_0+C_0),$$

where $\hat{M}_s(\omega)$ is the revolution matrix from point $s_0$ to point $s_0+C_0$. This matrix includes the kick effect of feedback:

$$\hat{M}_s(\omega)=\hat{D}^{-1}\hat{M}(\omega)\hat{D};$$

$$\hat{M}(\omega)=\hat{M}_0+\frac{1}{\sqrt{\beta_P\beta_K}}K_T(\omega)\exp\left(j\omega(\tau_{PK}-\tau)\right)\hat{A}_0\hat{T}. \qquad (18)$$

Here $\hat{M}_0$ is the unperturbed revolution matrix from point $s_P$ on the closed orbit ($s_P$ is the PU location). Hence, the solution for $\hat{y}_0(\omega,s_0)$ is

$$\hat{y}_0(\omega,s_0)=\left(\exp(j\omega T_0)\hat{I}-\hat{M}_s(\omega)\right)^{-1}\cdot\hat{y}_{f0}(\omega,s_0+C_0).$$

Now we should remember that $s_0$ is an arbitrary point. Hence, after obvious transformations on the inverse matrix we find from the last solution for $\hat{y}_0(\omega,s_0)$ the general solution of Eq.(13) which satisfies (16) for an arbitrary point s:

$$\hat{y}(\omega,s)=\frac{\exp(j\omega T_0)\hat{I}-\hat{M}_s^{-1}(\omega)\cdot\det\hat{M}_s(\omega)}{\det\left(\exp(j\omega T_0)\hat{I}-\hat{M}_s(\omega)\right)}\hat{y}_f(\omega,s), \qquad (19)$$

where

$$\tilde{Y}_f(\omega,s)=\int_s^{s+C_0}\left[V_0^{-2}(j\omega x_c(0,s') + \dot{x}_c(0,s'))+\frac{F(s')}{j\omega}\right]\exp\left(\frac{j\omega s'}{V_0}\right)\cdot$$

$$\cdot\sqrt{\beta(s)\beta(s')}\sin\left(2\pi Q(\omega)+\psi(s)-\psi(s')\right)ds'.$$

The complex value $2\pi Q(\omega)$ depends on the tune at frequency $\omega/2\pi$. It is clear from (19) that the general solution in time domain variables is fully determined by the eigen frequencies $\omega_k$, that is the solutions of the following equation:

$$\det\left(\exp(j\omega T_0)\hat{I}-\hat{M}_S(\omega)\right)=\det\left(\exp(j\omega T_0)\hat{I}-\hat{M}(\omega)\right)=$$

$$=\exp(j2\omega T_0)-\exp(j\omega T_0)\mathrm{Tr}\hat{M}(\omega)+\det\hat{M}(\omega)=0, \qquad (20)$$

where $\mathrm{Tr}\hat{M}(\omega)$ is the trace of the matrix $\hat{M}(\omega)$. The motion of the particles will be stable if

$$\mathrm{Im}\omega_k > 0. \qquad (21)$$

It is easy to see that Eq.(20) and the stability condition (21) are in accordance with the same equations in [10,12] which have been obtained for ImQ=0. But equation (20) has a more general sense and may be used when |ImQ|>0. Due to the formal accordance between Eq.(20) and similar equations in [10] or [12] we can say that the results from [10,12] may also be used when |ImQ|>0.

When $K_T(\omega) = 0$ in (18), we have for $\omega_k$ from (20)

$$\omega_k = \left(n_k \pm Q(\omega_k)\right)\omega_0, \qquad (22)$$

where $n_k$ - integer (positive or negative). We shall use further the agreement that for k = 1 the $n_1$ value is the nearest integer to ReQ. Eq.(22) is well known in the theory of resistive wall instability.

Now we make some assumptions for $\hat{M}(\omega)$ in (18) in order to simplify our formulas. Let us assume $\beta'_P = 0$ and $\tau_{PK}=\tau$; these assumptions are usually valid in an accelerator. Then we get:

$$\hat{M}(\omega)=\hat{M}_0+\frac{1}{\sqrt{\beta_P\beta_K}}K_T(\omega)\hat{A}_0\hat{T}; \qquad (23)$$

$$\mathrm{Tr}\hat{M}(\omega)=2\cos(2\pi Q)+K_T(\omega)\sin\left(2\pi Q(\omega)-\psi_{PK}\right), \quad \det\hat{M}(\omega)=1-K_T(\omega)\sin(\psi_{PK}),$$

where $\psi_{PK}$ is a complex value, the real part of which is the phase advance from PU to DK. Therefore, from (20) we get:

$$\exp(j\omega_k T_0)=\cos\left(2\pi Q(\omega_k)\right)+\tfrac{1}{2}K_T(\omega_k)\sin\left(2\pi Q(\omega_k)-\psi_{PK}\right)\pm$$

$$\pm j\sqrt{\left[\sin\left(2\pi Q(\omega_k)\right)-\tfrac{1}{2}K_T(\omega_k)\cos\left(2\pi Q(\omega_k)-\psi_{PK}\right)\right]^2-\tfrac{1}{4}K_T^2(\omega_k)}. \qquad (24)$$

This formula will be analyzed further.

The asymptotic behavior of the solution (19) for $t\to\infty$ can easily be known with the formula:

$$\lim_{t\to\infty} x_c(t,s) = \lim_{\omega\to 0} j\omega\, \tilde{x}_c(\omega,s).$$

Of course, this relation is valid if the limit exists. For example, when $K_T=0$ we have from (19):

$$\lim_{t\to\infty} x_c(t,s) = \lim_{\omega\to 0} j\omega\, \tilde{x}_c(\omega,s) = \lim_{\omega\to 0} j\omega\, y(\omega,s)\, \exp(-j\omega s/v_0) =$$

$$= \frac{1}{2\sin(\pi Q)} \int_s^{s+C_0} F(s')\sqrt{\beta(s)\beta(s')}\cos\big(\pi Q+\psi(s)-\psi(s')\big)ds'. \tag{25}$$

This is the well known formula for the closed orbit when we have a perturbation in the magnetic guide field.

## 4 THE IDEAL FEEDBACK

The ideal feedback corresponds to a wide band amplifier without filter ($K_f=1$). In this case the amplitude and phase characteristics $K_V$ of the feedback circuit depend weakly on frequency. If $K_T(\omega)$ depends weakly on frequency

$$\left|\frac{\omega}{K_T}\frac{dK_T}{d\omega}\right| \ll 1, \tag{26}$$

then we can consider $K_T$ as a parameter. Let us assume that the condition (26) is also valid for $Q(\omega)$. Then for $|K_T|\ll 1$ we can write from (24):

$$\exp(j\omega_k T_0) \cong \exp\big(\pm j2\pi Q(\omega_k)\big)\left(1 \mp j\,\frac{1}{2}\,K_T(\omega_k)\exp(\mp j\psi_{PK})\right). \tag{27}$$

Hence, we get the damping time $\tau_D$:

$$T_0/\tau_D = -\mathrm{Im}(\omega_k T_0) = \frac{1}{2}|K_T(\omega_k)|\sin(\mathrm{Re}\psi_{PK})\cos(\varphi) - 2\pi|\mathrm{Im}Q(\omega_k)|, \tag{28}$$

where $\varphi=\arg(K_T)$. This decrement formula is well known [8].

We see from (28) that the best damping will be for the ideal amplifier with:

$$|\cos(\varphi)| = 1$$

or $K_T$ real and for PU and DK locations such that:

$$|\sin(\mathrm{Re}\psi_{PK})| = 1,$$

i.e. if the phase advance $\psi_{PK}$ from PU to DK is equal to an odd number of $\pi/2$ radians. In this situation the PU and DK are separated by an odd number of quarter $\beta$-oscillations. For such positions the oscillations will be damped if the gain is

$$|K_T| > 4\pi|\text{Im}Q|. \tag{29}$$

Hence, for LHC we must ensure $|K_T| > 0.4$ if $|\text{Im}Q| = 0.03$.

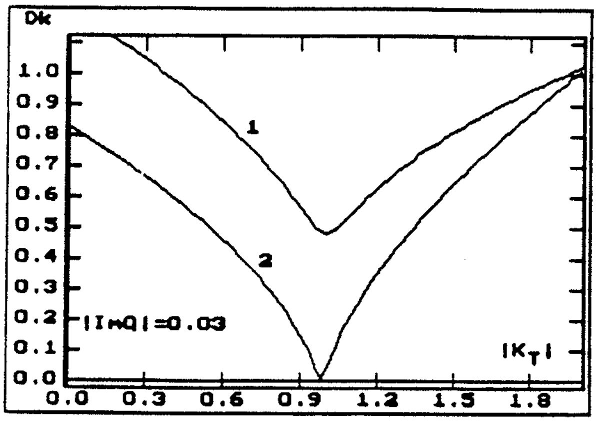


Fig.2

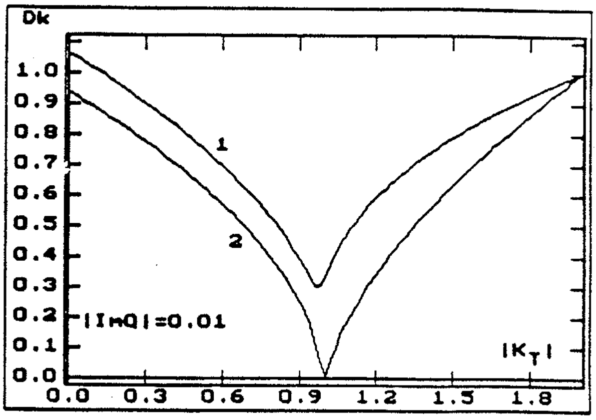


Fig.3

The dependence of the damping factor $D_k$:

$$D_k = \exp(-\text{Im}\omega_k T_0) = \exp(-T_0/\tau_D), \qquad k = 1, 2 \tag{30}$$

on the gain $|K_T|$ is shown for the two cases $|\text{Im}Q| = 0.03$ (Fig.2) and $|\text{Im}Q| = 0.01$ (Fig.3). These curves correspond to the two solutions of (24) with $|\cos(\varphi)| = 1$ and $|\sin(\text{Re}\psi_{PK})| = 1$. One sees that the curves agree with the analytical solutions (28) and (29) for $|K_T| \ll 1$. The minimum damping time $\tau_D = 1.55T_0$ corresponds to $|K_T| = 1.02$ ($|\text{Im}Q| = 0.03$).

The damping time required is linked to machine non-linearities. It is known that the filamentation time due to tune spread $\Delta Q$ is [13]

$$\tau_f \approx T_0/(\pi\sqrt{2}\Delta Q).$$

For the LHC $\Delta Q \approx 0.005$. Hence, $\tau_f \approx 45T_0$. We shall assume that a damping time of 10 revolution periods should be sufficient to overcome filamentation:

$$\tau_D \approx 10T_0 \ll \tau_f.$$

This corresponds to an amplitude decrease of 10% per revolution (or $D_1 < 0.9$ in Fig.2, 3) and gives (see Fig.2):

$$|K_T| = 0.54.$$

This is the gain needed for the transverse feedback in LHC.

In Fig.3, 4 the fractional part of $\mathrm{Re}Q_k$ is shown:

$$\{\mathrm{Re}Q_k\} = |\mathrm{Re}(\omega_k T_0/2\pi)|, \qquad k = 1,\ 2. \tag{31}$$

The eigen frequencies $\omega_k$ can be found from (27) taking into account the same agreement as in (22). One sees that increasing the gain increases also the fractional part of the coherent Q. For $|K_T| = 0.54$ and $|\mathrm{Im}Q| = 0.03$ this increase is equal to 0.004.

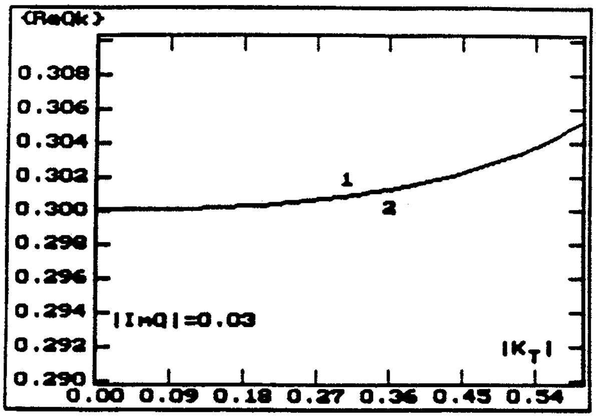


Fig.4

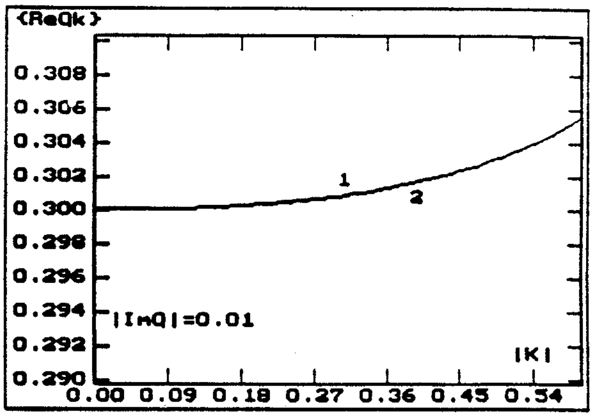


Fig.5

If we assume that the initial error is estimated to [1]:

$$|x_p| \le 0.5 \text{ mm},$$

we can obtain the kicker strength from Eq.(9)

$$|\Delta x'_K| \cong \frac{1}{\sqrt{\beta_p \beta_K}} |K_T x_p| \cong \frac{1}{\beta_{max}} |K_T x_p| \le 1.6\ \mu\text{rad}, \tag{32}$$

where it has been assumed that $\beta_K = \beta_p = \beta_{max} = 165.8$ m. This kicker strength is approximately the same as in the SPS, but the beam energy at injection in LHC is in $450/26 \cong 17.3$ times higher than in SPS at injection. This means that the power for the LHC kicker must be correspondingly higher.

## 5 THE FEEDBACK WITH DIGITAL IIR-FILTER

Filters in the feedback circuits are used to suppress the revolution harmonics in the PU signal. The FIR-filters (finite duration impulse response filter) are widely used now [8,9], but they decrease significantly the stability region [4,5,12]. On the other hand IIR-filters (infinite duration impulse response filter) have better characteristics [7,10] and their use for LHC will be analyzed in the following.

One of the forms of an IIR-filter is shown in Fig.6. This filter consists of non-recursive circuits with amplifiers $a_m(\omega)$, recursive circuits with amplifiers $b_m(\omega)$ and delays $T_0$. The order the filter is $p$. For this filter we can write:

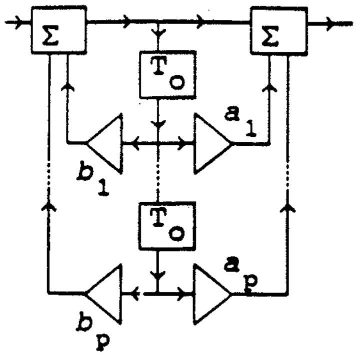


Fig.6

$$K_T(\omega) = K(\omega)\frac{1+\sum_{m=1}^{p} a_m(\omega)\exp(-jm\omega T_0)}{1-\sum_{m=1}^{p} b_m(\omega)\exp(-jm\omega T_0)}. \qquad (33)$$

We must remember that an FIR-filter consists of non-recursive circuits only, with $b_m = 0$. Let us assume that condition (26) is valid for $K(\omega)$, $a_m(\omega)$ and $b_m(\omega)$. Substituting $K_T(\omega)$ from (33) into (20) we get for $\exp(j\omega T_0)$ an equation of order (p+2). Hence, one will find additional beam oscillation modes for the damper system with IIR-filter.

Some results for the IIR-filter of first order ($p$=1) follow. In this case Eq.(20) becomes a cubic equation. If $|K(\omega)| \ll 1$, then in linear approximation we obtain:

$$\exp(j\omega_k T_0) \cong \exp(\pm j2\pi Q)\left(1\mp j\tfrac{1}{2}K(\omega_k)\exp(\mp j\psi_{PK})\right) -$$
$$- \tfrac{1}{2}(a_1+b_1)K(\omega_k)\left[1\pm j\left(\sin(2\pi Q-\psi_{PK}) + (b_1-\mu\cos(2\pi Q))/\sin(2\pi Q)\right)\right];$$

$$\exp(j\omega_k T_0) \cong b_1 + (a_1+b_1)\mu K(\omega_k), \qquad (34)$$

where

$$\mu = \left[b_1\sin(2\pi Q-\psi_{PK}) + \sin(\psi_{PK})\right]/\left[1 - 2b_1\cos(2\pi Q) + b_1^2\right].$$

We see from (34) that the first two solutions for $\exp(j\omega_k T_0)$ differ very little from the solutions of (28). The new third solution is the low frequency solution and significantly depends on the IIR-filter parameters. The third mode will be stable if $|b_1|<1$. This condition is the stability condition for the IIR-filter itself.

The $a_1$ parameter must be equal to -1 because we shall have the solution (25) for the closed orbit if

$$K_T(\omega=0) = 0.$$

This gives for (33):

$$\sum_{m=1}^{p} a_m = -1 \qquad (35)$$

and $a_1$=-1 for $p$=1. This condition means also that the revolution harmonics with frequency $mf_0$ will be suppressed completely.

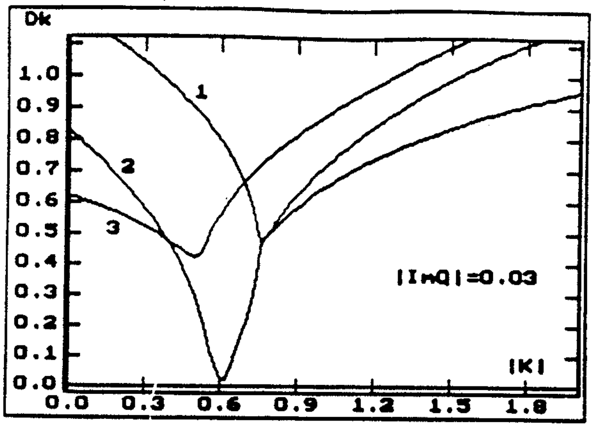


Fig.7

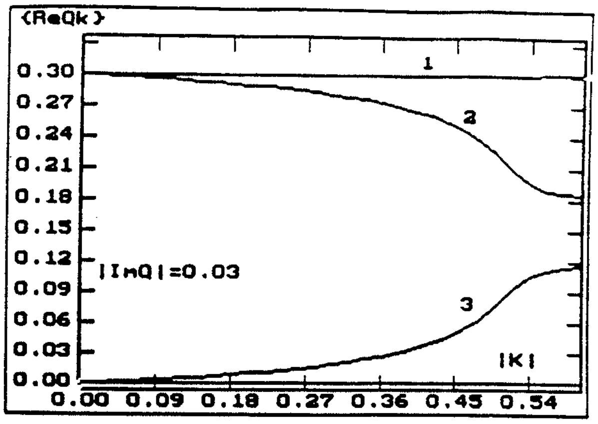


Fig.8

The dependences of the damping factor $D_k$ (30) and of the fractional part $\{ReQ_k\}$ (31) on $|K|$ are shown in Fig.7 and Fig.8 respectively. The PU and DK locations are such that $Re\psi_{PK}$ is equal an odd number of $\pi/2$ radians (for such PU and DK positions the damping factor $D_k$ is the best for an ideal feedback). All curves have been calculated by the Cardan formula for Eq.(20) with $ReQ = 70.3$, $|ImQ| = 0.03$, $a_1 = -1$ and $b_1 = 0.62$.

The curves 1 and 2 correspond to the eigen frequencies with the number of oscillations per turn in the neighborhood of ReQ. Curve 3 corresponds to the third root of Eq.(20). This oscillation mode is determined by the filter structure and is in accordance with the approximate formula (34). For a small gain the damping time $\tau_D$ is determined by curve 1. For example, if $|K| = 0.50$ then $\tau_D \cong 10T_0$ (corresponds to $D_1 = 0.9$).

It is necessary to emphasize that the damping time $\tau_D$ and the stability region for $|K|$ are limited by the first mode (for a small $|K|$) and the third mode (if $|K|$ is large). Hence, the $\tau_D$ values are determined by region between curves 1 and 3 in Fig.7. The best damping corresponds to the cross point of curves 1 and 3. This value depends on $|ImQ|$ and $b_1$.

The parameter $b_1$ was chosen to optimize the damping factor obtained from the curves $MAX(D_k(b_1, |K|))$, $k = 1, 2, 3$. These curves are shown in Fig.9a. One sees that for $|ImQ| = 0.03$ the best damping corresponds to $b_1 = 0.62$. In this case $|K| = 0.50$ for $D_1 = 0.9$. In Fig.9b the transfer function of the filter is shown. One sees that $|K_f(\omega_{min} \cong 0.3\omega_0)| = 1.22$ for $b_1 = 0.62$.

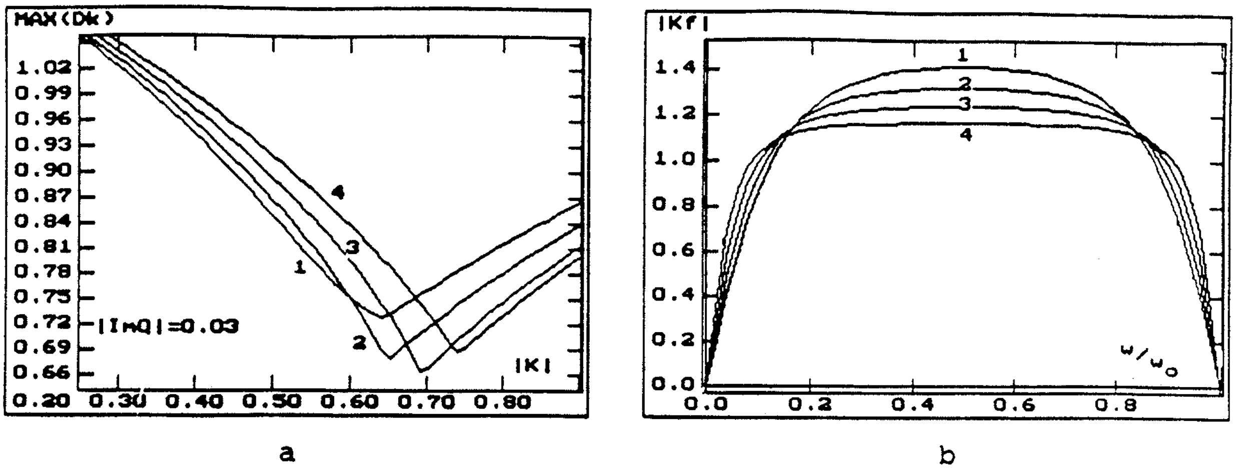


Fig.9. (a) MAX($D_k$) versus $|K|$ and (b) $|K_f|$ frequency response versus $\omega/\omega_0$ for $b_1$= 0.32+0.1n; n=1,..4. The curve labels are n-values.

The optimum value for $b_1$ depends on |ImQ|. For example, if |ImQ| = 0.01 then $b_1$= 0.66. For this case the dependences of $D_k$ and of {$ReQ_k$} on $|K|$ are shown in Fig.10 and Fig.11 respectively. One sees that $|K|$ = 0.30 for $D_1$= 0.9.

From these results it follows that in the filter design it is useful to foresee the possibility to vary $b_1$.

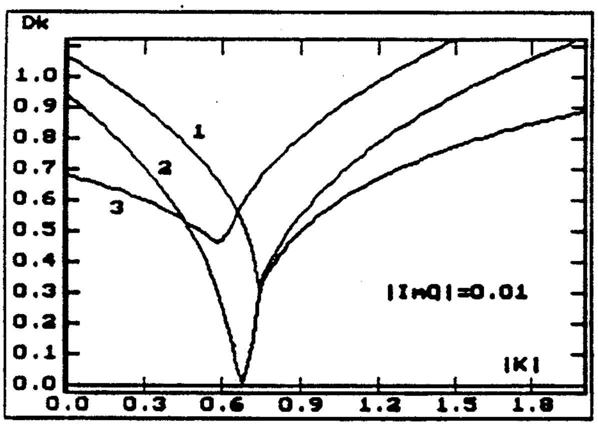


Fig.10

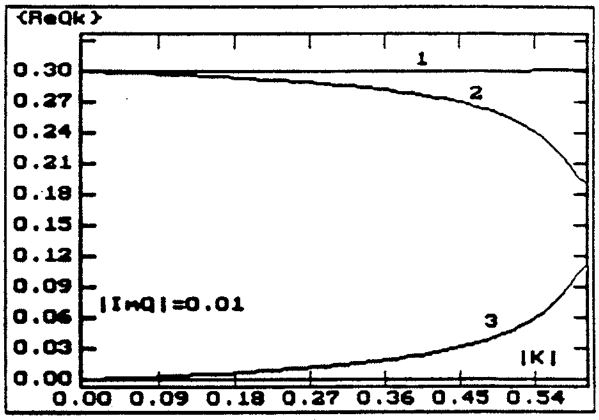


Fig.11

The other important peculiarity of the damper system with IIR-filter is shown in Fig.8, 11. One sees that the difference between {$ReQ_k$} (k= 1, 2 3) is not small. For example, if |ImQ| = 0.03 then the coherent frequencies are $0.30\omega_0$; $0.22\omega_0$ and

$0.08\omega_0$ for $|K| = 0.50$ ($D_1 = 0.9$). However, the presence of more than two transverse oscillation modes does not prevent the use of such a damper system: all these modes are damped oscillations in the stability region. Nevertheless, possible parametric resonances of such a damper system must be studied (the problem for external resonances is shortly discussed in [6]).

## 6 CONCLUSION

The following Table contains the main parameters to be proposed for the LHC damper system without and with an IIR-filter of the first order in the feedback circuit. All values are shown for the gain $|K_T|$ or $|K|$ corresponding to $D_1 = 0.9$.

Table

| Parameter | ImQ = 0 | \|ImQ\| = 0.01 | \|ImQ\| = 0.03 |
|---|---|---|---|
| **Ideal feedback** | | | |
| $\|K_T\|$ ($D_1 = 0.9$) | 0.19 | 0.31 | 0.54 |
| $\|\Delta x'_K\|$ ($\mu$rad) | 0.57 | 0.93 | 1.63 |
| **Feedback with IIR-filter** (p = 1) | | | |
| $b_1$ | 0.67 ≅ 86/128 | 0.66 ≅ 84/128 | 0.62 ≅ 79/128 |
| $\|K\|$ ($D_1 = 0.9$) | 0.18 | 0.30 | 0.50 |
| $\|K_f(\omega_{min})\|$ | 1.18 | 1.19 | 1.22 |
| $\|K_T\|$ | 0.21 | 0.36 | 0.61 |
| $\|\Delta x'_K\|$ ($\mu$rad) | 0.64 | 1.08 | 1.84 |

**Acknowledgements**

The author wishes to thank Dr. D.Boussard (CERN) for help and very fruitful discussions.

## REFERENCES


[1] Design Study of the Large Hadron Collider (LHC). CERN 91-03, Geneva, 2 May 1991.

[2] V.I.Balbekov. - Space Charged Effects in UNK. In: The IX All Union Conference on Particle Accelerators. JINR, Dubna, 1985, vol.2, p.360 (in Russian).

[3] V.I.Balbekov, K.F.Gertsev. - The Feedback System for Damping of Resistive Instability in UNK. IHEP 87-120, Serpukhov, 1987 (in Russian).

[4] V.M.Zhabitsky. - The Z-Transform Application for Solving the Problem of Free Beam Oscillation Damping in the Accelerator. JINR P9-91-91, Dubna, 1991 (in Russian).

[5] V.M.Zhabitsky, I.N.Ivanov, I.L.Korenev, L.A.Yudin. - Damping of Resistive Instability in UNK-I with Digital Electronics in Feedback. JINR P9-91-99, Dubna, 1991 (in Russian).

[6] V.M.Zhabitsky, I.L.Korenev, L.A.Yudin. - The Stability of the Damper System for Coherent Transverse Oscillations of the Beam in Synchrotron. JINR P9-91-246, Dubna, 1991 (in Russian).

[7] V.M.Zhabitsky, I.L.Korenev, L.A.Yudin. - The Resistive Instability Damper System for the First Stage of the UNK Accelerator with IIR-Filter in Feedback. JINR P9-91-494, Dubna, 1991 (in Russian).

[8] E.Ebert et al. - Transverse and Longitudinal Multi-Bunch Feedback Systems for PETRA. DESY 91-036, 1991.

[9] L.Vos. - Transverse Feedback System in the CERN SPS. CERN SL/91-40 (BI), Geneva, 1991.

[10] V.M.Zhabitsky. - The Transverse Damper System with Digital Feedback and a New Method to Study It. Report at CERN Accelerator School. Netherlands, September, 1991.

[11] B.Zotter, F.Sacherer. - Transverse Instabilities of Relativistic Particle Beams in Accelerators and Storage Rings. In: Theoretical Aspects of the Behaviour of Beams in Accelerators and Storage Rings. CERN 77-13, Geneva, 1977, p.198.

[12] V.M.Zhabitsky. - Theoretical Treatment of a Classical Transverse Feedback System Using Z-Transform. JINR E9-91-156, Dubna, 1991.

[13] Brouzet E. et al. - A Damper for $\bar{p}$ Injection Oscillations in the PS Machine. IEEE Trans. Nucl. Sci., NS-32, No.5, p.2135 (1985).